

Date of publication xxxx 00, 0000, date of current version xxxx 00, 0000.

Digital Object Identifier 10.1109/ACCESS.2017.DOI

Agent-Based Modelling of Malaria Transmission

BABAGANA MODU^{1*}, SAVAS KONUR² and POLOVINA NEREIDA³

¹Department of Mathematics and Statistics, Yobe State University, Damaturu, Nigeria, (e-mail: bmodu@ysu.edu.ng)

²Department of Computer Science, University of Bradford, UK, (e-mail: s.konur@bradford.ac.uk)

³Manchester Metropolitan Business School, Manchester Metropolitan University, UK (e-mail: n.polvina@mmu.ac.uk)

*Corresponding author: Babagana Modu (e-mail: bmodu@ysu.edu.ng).

B. Modu's work was supported by the Tertiary Education Trust Fund (Tetfund) Nigeria (in collaboration with Yobe State University Damaturu) for sponsoring his PhD studies at the University of Bradford. S. Konur was supported by EPSRC (EP/R043787/1).

ABSTRACT Despite global efforts to eradicate malaria, it remains a major health threat to nearly half of the world's population. Recent statistics show that globally, there are over 200 million malaria cases, and estimated deaths are close to half a million. Africa alone accounts for almost 90% of these cases. Numerous studies have been conducted to understand the transmission dynamics of malaria. Mathematical methods have been widely used to model and understand disease dynamics and outbreak patterns. Although mathematical methods have provided good results for homogeneous populations, they impose significant limitations for investigating certain heterogeneities in a population, such as age and vaccine status. This paper proposes an agent-based modeling approach that permits the capture of heterogeneous mixing and agent interactions, thus enabling a better understanding of malaria dynamics and outbreak patterns. Our approach is illustrated in a case study using climate and demographic data of the cities of Tripura, Limpopo, and Benin. Our agent-based simulation was validated against the reported cases of malaria collected in these cities. Furthermore, the efficiency of the proposed model was compared with the mathematical models used as a benchmark. A statistical test confirmed that the agent-based model is robust and has the potential to accurately predict the peak seasons of malaria. These results can help healthcare providers and policymakers have intervention mechanisms in place in advance, which can potentially help reduce the malaria transmission rate.

INDEX TERMS Agent-based modelling, Mathematical modelling, Simulation, Malaria, Climate factors, *NetLogo*, *VenSim*

I. INTRODUCTION

DESPITE continuous efforts by the World Health Organization (WHO) and other healthcare organizations, malaria remains a global health threat. More than 200 million cases and approximately half a million deaths are reported annually as a result of malaria. The African continent alone accounts for almost 90% of reported cases [1]–[3]. In addition to the poor healthcare facilities in Africa, the lack of efficient intervention mechanisms for the planning and management of disease outbreaks remains a key challenge. In this respect, prior information on the likelihood of a malaria outbreak and accurate prediction of the outbreak times can be crucial for taking the necessary steps in time. One of the most crucial aspects of modeling disease outbreaks is the generation of an appropriate realistic model. Traditionally, models mostly used for epidemic studies have

been developed using either equation-based (mathematical) or simulation-based (e.g., agent-based) approaches. Both modelling approaches have advantages and disadvantages, and deciding which model is appropriate depends on each approach's comparative advantages and ability to successfully model a disease outbreak. In epidemiology, equation-based models are generally used to describe the disease progression. For instance, several studies (e.g., [4]–[10]) have been conducted using compartmental modelling techniques through equation-based models to model and understand disease transmission dynamics. These models were useful to investigate the disease progression from a population perspective by characterizing individuals according to their health status (e.g., 'susceptible', 'infected' and 'recovered'). Although compartmental models are powerful methods for investigating disease dynamics, they assume that human

populations are homogeneous [11]. Human populations are heterogeneous and are influenced by a wide spectrum of factors, including age, sex, spatial and temporal changes, human movement patterns, and social network patterns [12]. However, the models are designed for homogeneous populations, adding new factors to the population requires introducing additional equations within the model, thus making the model more complex and inefficient. In addition, equation-based models assume homogenous mixing, where each agent has an equal probability of coming into contact with every other agent. This limitation makes compartmental models inadequate for capturing the heterogeneities arising from different factors, such as contact rate, death rates, and length of incubation periods among each agent in a population.

Discrete-event simulation models have also been used to investigate and understand the spread of infectious diseases using probabilistic models. For instance, [13] used a data-driven global stochastic epidemic model to analyze both the spatial and temporal dynamics of the Zika virus spread in the Americas. The model estimates the time and place of the first Zika case, the rate of attack, the duration of the epidemic, and the expected number of newborns to be infected. In another study, [12], [14]–[16] used a continuous-time hidden Markov model to study the dynamics of cholera based on environmental factors, such as water depth and water temperature. The developed model can predict the number of infected individuals in the population weeks before cholera cases were observed. In addition to the prediction capabilities of discrete-event simulation models, they are useful for investigating various intervention strategies [17]. Discrete-event models are capable of determining the intuitive characteristics (e.g., length of transmission, reproduction rate, occurrence rate, etc.) of an outbreak. However, this approach is inefficient because it is unable to study the counterintuitive behaviour of individuals on the overall impact of disease spread.

To overcome these limitations, we propose an agent-based modelling approach to capture heterogeneity in the context of malaria transmission and especially in a mosquito population. This includes the length of the incubation period, the lifespan of mosquitoes, the birth rate and the rate at which eggs are deposited. Agent-based models (ABMs) are computational modelling tools consisting of agents that communicate with each other within their environment and behave according to a set of pre-defined rules. ABMs are powerful because of their stochasticity, spatial explicitness, and discrete-time-based simulations, where each agent interacts in space and time [18]. ABMs accurately represent increased stochasticity in low-transmission settings, high-resolution spatial simulations and heterogeneities [19]. ABMs often work as a bottom-up modelling approach as population-based behaviour emerges from interactions among autonomous agents [20], [21]. These aspects make ABMs a flexible modelling technique for consolidating heterogeneous variables (e.g., host movement and heterogeneous implementation interventions) and stochasticity (e.g., inter-patient variability at the time of infection, time to recovery, and the location

of infection) [19], [22]–[24]. Furthermore, ABMs allow a high degree of heterogeneity in the creation, disappearance, and movement of a finite collection of discrete interacting individuals [20]. The stochasticity of ABMs permits variation due to randomness, and thus, more accurately mimics the transmission of malaria, thereby reducing the effects of systematic preference among the agents [19]. The agent-based malaria transmission models developed in this study enable us to investigate not only individual agent behaviour but also how they communicate with each other according to some rules and their responses to climate factors. Agent-based models were utilized to simulate actual malaria cases in Tripura, Limpopo, and Benin using the climate and demographic data obtained for these cities. Hence, emerging results were used to validate the actual reported cases in these cities. Statistical tests were also performed to evaluate the accuracy of the proposed model.

A. ACHIEVEMENTS, CONTRIBUTION, AND ORIGINALITY

This paper is a part of a PhD research [25], addresses the limitations of the previous works, e.g., [6], [8], [26]–[28], by developing a new mathematical model that introduces a temperature-dependent incubation state into the exposed mosquito population (see Figure 1). This state is critical for developing effective prevention and control mechanisms, which should not only focus on controlling human infection, but also the mosquito. The models presented in [6], [8], [26]–[28] assumed that human and mosquito populations are homogeneous, and thus inadequate for capturing heterogeneities, such as contact rate, death rates, and length of incubation periods among each agent in a population. The contribution of this study is the development of an agent-based model to capture the heterogeneities among individual agents, which lacks a mathematical approach. Using a case study, we have shown that agent-based modelling performs better than mathematical modelling. We also generated a location-specific malaria transmission model by using demographic and climate-specific parameters and data. This model can be easily adapted for different regions and locations to predict malaria transmission trends and patterns and could be a valuable tool for healthcare providers to assist in developing intervention strategies.

B. ORGANIZATION

The remainder of this paper is organized as follows: In Section II, the malaria transmission framework, together with agent-based and mathematical modelling approaches, is discussed. Section III describes the methodologies. Section IV presents the simulation results. Section V presents and discusses the results. The conclusions and future work are summarized in Section VI.

II. MODEL FORMULATION

This section provides a theoretical background of compartmental modelling, agent-based modelling, and their applica-

tion to the study of malaria. The malaria transmission model shown in Figure 1 was developed based on the model by [6], where the incubation period in a human was investigated. However, developing mechanisms for mitigating the malaria threat should not only focus on controlling human infection but also vector control as this is important for developing prevention and control strategies. Hence, we fill this gap by introducing a temperature-dependent incubation state into the exposed mosquito (see the dotted black circles in Figure 1 against the aquatic and exposed mosquito). The red arrows indicate the malaria infection transfer rate from human to mosquito and vice-versa, while other colours indicate transition rates from compartment to compartment.

Our model captures the dynamics of both human and mosquito populations, and the temperature-dependent parameters of the model are defined in Section III. (see Table 1 for the definition of the parameters). Malaria spreads among human populations through anopheles mosquito bites (female-type). Figure 1 presents the compartments describing human and mosquito dynamics, in which human dynamics are structured using SEIR (susceptible, exposed, infected, and recovered) attributes, and mosquito dynamics are structured using ASEI (aquatic, susceptible, exposed, and infected) attributes. The temperature was incorporated into the model to analyze its effect on the biting rate, survival rate, parasite development, juvenile maturation rate, and mortality rate.

TABLE 1. Model parameters and their definitions.

| Description of the parameter used | Symbol |
|---|-------------------------------|
| Human recruitment rate | η |
| Human immunity loss rate | ω_h |
| Human death rate | μ_h |
| Death rate of adult female mosquitoes | $\mu_m(T)$ |
| Death rate of aquatic mosquitoes | $\mu_a(\hat{T})$ |
| Egg deposition rate by adult female mosquitoes | $\alpha_E(T, \hat{T})$ |
| Transition probability | p |
| Transfer rate of exposed humans to infected class | α_h |
| Recovery rate for infectious humans to malaria infection | γ_h |
| Transfer rate of infected mosquitoes undergoing latent period | $\theta_m(T)$ |
| Delay due to malaria parasite incubation period | $\tau_{EIP}(T) = \tau_2$ |
| Malaria transfer from infected mosquitoes to susceptible humans | a |
| Malaria transfer from infected humans to susceptible mosquitoes | b |
| Biting rate of mosquitoes on susceptible humans population | c_m |
| Ratio of mosquitoes population to humans population | m |
| Recruitment rate of adult female mosquitoes | $\phi_{EA}(T, \hat{T})$ |
| Carrying capacity of immature mosquitoes | K_c |
| Delay due to maturation rate of immature mosquitoes | $\tau_{EA}(\hat{T}) = \tau_1$ |
| Malaria induced death rate of infected humans | δ_h |
| Extrinsic incubation period | $EIP(T)$ |

A. MATHEMATICAL MODEL

A compartmental model is a mathematical modelling technique that has long been used to investigate epidemics. The ‘classical model’ [29] was the first mathematical technique that appeared in the literature that studied malaria transmission. Since then, several remarkable extensions have been made (e.g., [4]–[10], [30]–[33]) that build upon this model to address various emerging problems. In the mathematical modelling of malaria, a compartmental model (Figure 1) was used to describe the disease transition using a set of

differential equations [34]. The population within a particular compartment in a disease transmission model is assumed to be homogeneous and well-mixed based on health status, for example, ‘susceptible’, ‘infectious’, and ‘recovered’. Hence, each compartment of the disease transmission model was defined by its differential equations [35]–[37]. As shown in Figure 1, the human population is split into four compartments, depicted by the rectangular boxes labelled S_h, E_h, I_h, R_h denoting ‘susceptible’, ‘exposed’, ‘infectious’ and ‘recovered’ humans, respectively. Similarly, the mosquito population is split into five compartments that include its juvenile stages, labelled $A_m, S_m, E_m^s, E_m^l, I_m$ denoting ‘aquatic’, ‘susceptible’, ‘short-term exposed’, ‘long-term exposed’ and ‘infectious’, respectively. Moreover, the terms ‘short’ and ‘long-term exposed’ are used to describe the impact of temperature (as an environmental factor) on mosquitoes undergoing extrinsic incubation periods (i.e., the time it takes for parasites to develop in the mosquito from point of ingestion via an infected blood meal). The differential equations describing the transition within the compartments in Figure 1 are as follows:

$$\begin{cases} \dot{S}_h(t) = \eta - \Gamma_6 - \mu_h S_h(t) + \omega_h R_h(t) \\ \dot{E}_h(t) = \Gamma_6 - [\alpha_h + \mu_h] E_h(t) \\ \dot{I}_h(t) = \alpha_h E_h(t) - [\mu_h + \delta_h + \gamma_h] I_h(t) \\ \dot{R}_h(t) = \gamma_h I_h(t) - [\mu_h + \omega_h] R_h(t) \\ \dot{A}_m(t) = \Gamma_4 - \mu_a(T) A_m(t) - \Gamma_5 \\ \dot{S}_m(t) = \Gamma_5 - \Gamma_2 - \mu_m(T) S_m(t) \\ \dot{E}_m^s(t) = p \Gamma_2 - \Gamma_1 E_m^s(t) \\ \dot{E}_m^l(t) = (1 - p) \Gamma_2 - \mu_m(T) E_m^l(t) \\ \dot{I}_m(t) = \theta_m(T) E_m^s(t) + (1 - p) \Gamma_3 - \Gamma_7 \end{cases} \quad (1)$$

where $\Gamma_3 = \lambda_b(T) \psi(\tau_2, \mu_m, T)$, $\Gamma_7 = \mu_m(T) I_m(t)$, $\Gamma_4 = \alpha_E(T) [1 - A_m(t)/K_c] N_A(t)$, $\Gamma_5 = \phi_{EA}(T) \varphi(\tau_1, \mu_a, \hat{T})$ and $\Gamma_6 = \lambda_a(T) S_h(t) I_m(t)$. We define the initial conditions of the system (1) state variables as: $S_h(0) > 0$, $E_h(0) \geq 0$, $I_h(0) \geq 0$, $R_h(0) \geq 0$, $A_m(0) > 0$, $S_m(0) = \phi_{sm}(t) > 0$, $E_m^s(0) \geq 0$, $E_m^l(0) \geq 0$, $I_m(0) = \phi_{im}(t) > 0$, where $\phi_{sm}(\theta)$ and $\phi_{im}(\theta)$ are continuous functions in which the parameter θ is positively defined on $[-\tau, 0]$. For convenience, we scale down some differential equations in the system (1) by replacing the terms $\varphi(\tau_1, \mu_a, \hat{T})$ and $\psi(\tau_1, \mu_a, T)$:

$$\begin{aligned} \varphi(\tau_1, \mu_a, \hat{T}) &= A_m(t - \tau_1(\hat{T})) e^{-\mu_a(T) \tau_1(\hat{T})} e^{-A_m(t - \tau_1(\hat{T}))} \\ \psi(\tau_1, \mu_m, T) &= S_m(t - \tau_1(T)) I_h(t - \tau_1(T)) e^{-\mu_m(T) \tau_1(T)} \end{aligned} \quad (2)$$

$\phi_{EA}(T)$, denoting the survival probability of an egg to become an adult mosquito, is defined by $\phi_{EA}(T) = -0.00924 \hat{T}^2 + 0.453 \hat{T} - 4.77$ [38]. The parameters, $\lambda_a(T) = bc_m(T) = abm$ and $\lambda_b(T) = ac_m(T)$ are malaria infection transmission rates from human to mosquito and vice versa respectively. In system (1) and equation (2), all the temperature-dependent parameters are presumed con-

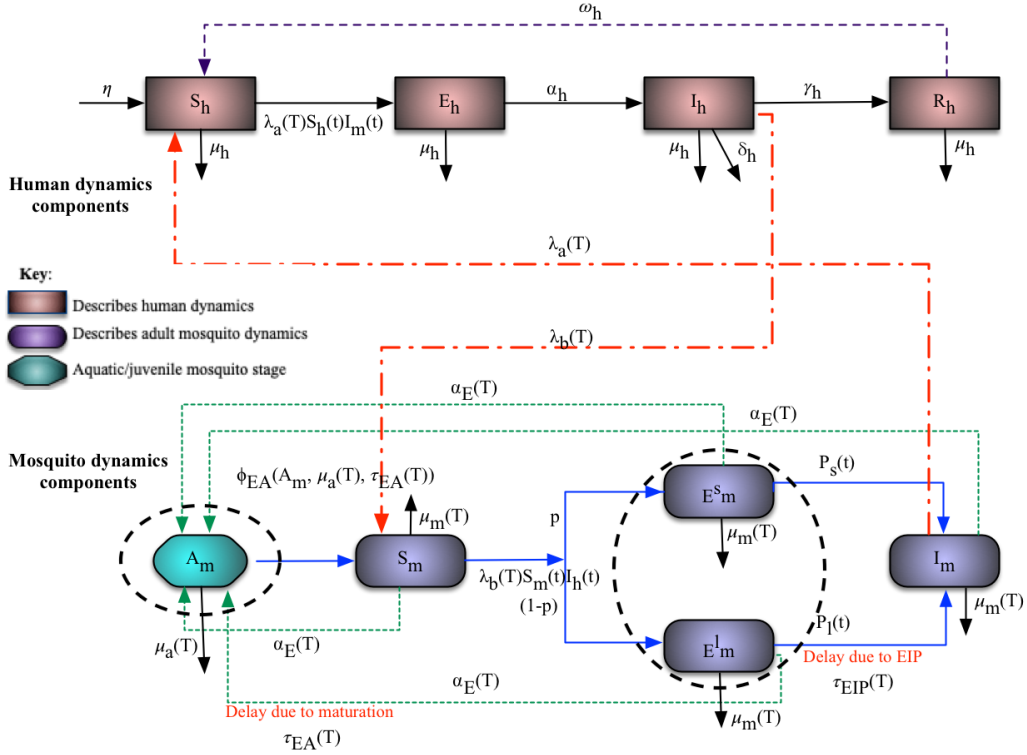


FIGURE 1. Malaria transmission diagram [25].

tinuous, bounded, positive and ω -periodic. As in [8], we also let $T = T(t)$ and $\hat{T} = T(t) + \delta_T$ to denote air and water temperature at time t . Table 1 presents the definition of the parameters in Figure 1, and their corresponding values, including their references, are presented in Table 3. The system of Equation (1) can be used to better understand the dynamics of malaria transmission. Moreover, mathematical models have proven to be suitable for modelling homogeneous systems at the macro scale rather than at fine granular levels (with heterogeneity).

To find the non-trivial disease-free state, we equate $E_h = I_h = R_h = E_m^s = E_m^l = I_m = 0$ in the system (1) which implies a disease-free equilibrium condition as

$$\mathcal{E}_o = (S_h^*, E_h^*, I_h^*, R_h^*, A_m^*, S_m^*, E_m^{s*}, E_m^{l*}, I_m^*), \quad (3)$$

$$= (\eta/\mu_h, 0, 0, 0, A_m^*(t), S_m^*(t), 0, 0, 0)$$

where $A_m^*(t)$ and $S_m^*(t)$ are the unique positive periodic solution of the system (1) and given by

$$\begin{aligned} \dot{A}_m(t) &= \Gamma_4 - \mu_a(T)A_m(t) - \Gamma_5 \text{ and} \\ \dot{S}_m(t) &= \Gamma_5 - \Gamma_2 - \mu_m(T)S_m(t). \end{aligned} \quad (4)$$

Hence, the local, asymptotically stability of the disease-free solution of equation (3) is solved by next generation operator [39]–[41].

B. AGENT-BASED MODELLING

In contrast to mathematical models, an agent-based model is generally characterized by a bottom-up approach. The agent-based approach enables individual agents to interact within their environment and behave according to predefined rules [42]. In addition, individual entities are represented by discrete autonomous agents communicating among themselves in a spatial environment to possibly produce non-intuitive emergent patterns at the population level [43]. Moreover, agent-based modelling represents purely rule-based algorithms, which start from scratch and continue until the desired model represents real-world phenomena of interest. In general, agent-based modelling is characterized by its ability to capture heterogeneity, spatial and complex interactions, microscale perspective, discrete-time considerations, and non-intuitiveness. All agents involved in the agent-based modelling of malaria transmission dynamics in Figure 1 (including their detailed descriptions) are presented in the following subsections.

1) Human Agents

Humans are among the agents responsible for malaria transmission. Infected humans can transmit malaria to susceptible mosquitoes through biting. Thereafter, the mosquito spreads malaria to a susceptible human by biting again. Once humans become infected with the malarial parasite, infection will not take place immediately until an intrinsic incubation period

is completed (incubation in humans). This period is called *intrinsic incubation period* (IIP), which refers to the starting time when an infected mosquito has successfully infected a susceptible human, and the pathogen has started to greatly increase in number inside the host body [44]. Subsequently, when the pathogen multiplies and reaches a certain threshold, malaria symptoms emerge. Furthermore, the chances of infection transmission are very high during this period. The IIP is presented in Figure 1 and illustrated as an exposed compartment in human dynamics. In essence, agent-based modelling captures the behaviour of individual agents and their interactions in the environment. The transmission of malaria is characterized by spatial and temporal properties, in which the movement of people, whether short- or long-term, supports the spread of malaria infection. People move from one place to another within their environment for different purposes. In this study, we also consider the movement of people within their local environment and thus observe emerging patterns. Although mosquitoes usually bite at night, other species bite during the day; however, our focus in this paper is to track infection-spreading patterns regardless of the time of day.

2) Mosquito Agents

The mosquito agent is a carrier of the malarial parasite and moves freely in search of humans to bite, thus transmitting the parasite. Naturally, mosquitoes have certain characteristics that compose their life cycle, including biting rate, mortality rate, egg deposition rate, birth rate, and immature mortality rate.

A potential malaria infection starts when a susceptible mosquito bites an infected human, after which the mosquito becomes infected with a probability of b . Conversely, when such an infected mosquito bites a susceptible human, it infects the human with probability a . Figure 1 illustrates the individual transitions in the compartments (SEIR) and their respective probabilities.

3) Pathogen Agents

The pathogen is a parasite that causes malaria infection and is called a *plasmodium species*. *Plasmodium* transfers to susceptible mosquitoes by biting an infected human and sipping blood containing the pathogen. Hence, the mosquito will become infected but not capable of transmitting the malaria infection to susceptible humans until the ingested blood containing the pathogen has the infection, that is until the various developmental stages before the mosquito becomes infectious. The time taken for the pathogen to complete its development inside the mosquito is called the *extrinsic incubation period* (EIP). This period is sensitive to environmental temperature [38], [45], [46], meaning that in a relatively high or low-temperature spectrum, the EIP could be shorter or longer, respectively.

4) Environment Agents

The environment, as an agent, leverages the spread of malaria and is constantly changing in space and time as the climate changes. The environment plays a vital role in the transmission of malaria and enables the movement of people and mosquitoes, providing mosquitoes with breeding sites for egg deposition and maturation of juvenile mosquitoes. To realistically simulate the spatial movement of humans and mosquitoes, an artificial environment was created using the *Netlogo* platform (see Figure 6), in which both humans and mosquitoes are displayed in the environment representing the spatial distribution of agents in a town, city, or community settlement.

III. MATERIALS AND METHODS

This section presents a detailed description of the methodology used in this study.

A. CASE STUDY

This study aimed to investigate the dynamics of malaria in human and mosquito populations using agent-based modelling. The developed model will be validated against reported malaria cases in different populations. To do this, we used data from three cities in different countries, including the Tripura district in India, Limpopo province in South Africa, and Benin city in Nigeria. These countries are known for their malaria endemic status [47] and have different seasons for transmission, climate patterns, parasites, and vector species. For instance, the Tripura district is known for its high malaria incidence, and the predominant species of the malaria parasite is *plasmodium falciparum*. This species alone accounts for approximately 90% of the reported cases, while *plasmodium vivax* comprises the remaining 10% of cases in the district [48]. In the Limpopo province, malaria is still endemic, as its incidence in the area is characterized by low altitude and climate [49], and it is connected to other regions in sharing boundaries with some parts of Zimbabwe and Mozambique, where malaria incidence is similarly high. Furthermore, the malaria season in Limpopo coincides with its warm and rainy summer that starts in September and continues through May the following year [50]. According to the World Health Organization (WHO), Nigeria is rated among the highest malaria-endemic countries worldwide [51]. Benin City is the capital of the state of Edo, located in the southern part of Nigeria. The city has a tropical climate, characterized by a long rainy season over 12 months, with an average annual temperature of 26.1°C. This rainfall pattern (with an average annual precipitation of 2025 mm) is regarded as the most likely influential climatic factor leading to the high incidence of malaria cases.

B. SOURCES OF DATA

The reported cases of malaria in Tripura, Limpopo, and Benin were taken from published sources [48], [52], [53], respectively. Because the occurrence of malaria is connected to climate factors, we need such data for the computation of

temperature-dependent parameters. In this study, we used the average monthly temperature, as the temperature is a large-scale driver of malaria transmission because it influences mosquito survival, parasite development, biting rate, and aquatic development of juvenile mosquitoes.

C. COMPLEXITY REDUCTION

Scaling down large populations is a common approach to reduce the complexity due to the computational resources required. ABMs are not expected to produce perfect predictions, but are accepted as abstractions and used to identify trends in behaviour of the simulated system under specific conditions. Therefore, the benefits of these complexity reductions in terms of runtime and data output may well outweigh any small inaccuracies in the simulation output [54].

The modelling and analysis of each selected city as a whole are computationally challenging because the cities shown in Figures 2–4 are too large in terms of population size and land size. Therefore, we scaled down the problem by defining “unit zones” to overcome the computational difficulties. In this particular experiment, the scaling down does not lead to a high level of inaccuracy. Since we do not have any data that represents local heterogeneity, we assumed the population density homogeneous across all regions of the cities in question. Using the population size of the cities and land mass, the population density of the cities can be obtained from $\rho = N/A$, where ρ = population density, N = total human population and A = total land area. Table 2 shows that all cities had different densities. For our analysis, the cities were scaled down according to their densities, and the consideration was to study the areas covering the dimensions of $1\text{km} \times 1\text{km}$ in Tripura, $3\text{km} \times 3\text{km}$ in Limpopo, and $1\text{km} \times 1\text{km}$ in Benin (Figures 2–4). Based on the reduced dimensions of the cities, as shown in Figures 2–4, the sub-populations of the demarcated areas were 1:35 (representing 350 people), 1:4 (representing 400 people), and 1:13 (representing 1300 people).

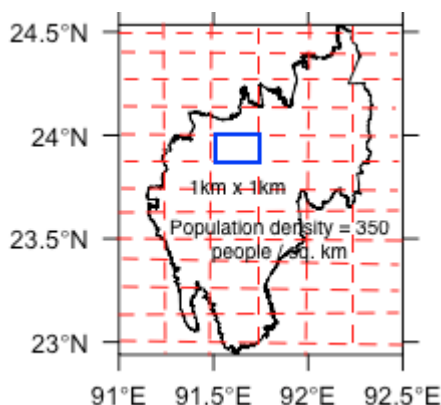


FIGURE 2. Illustrates the scaled down area of Tripura.

We also performed a local sensitivity analysis to determine the optimal scale to use. This follows by consid-

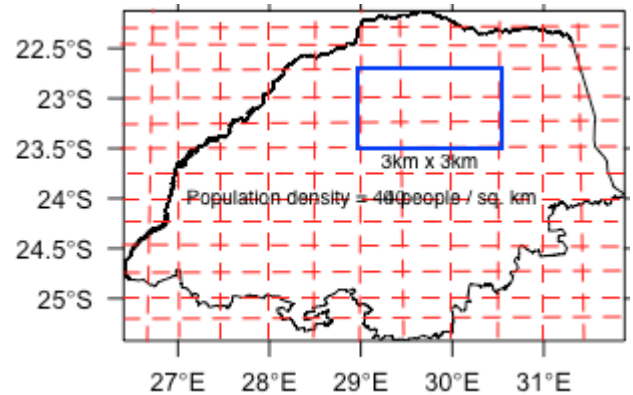


FIGURE 3. Illustrates the scaled down area of Limpopo.

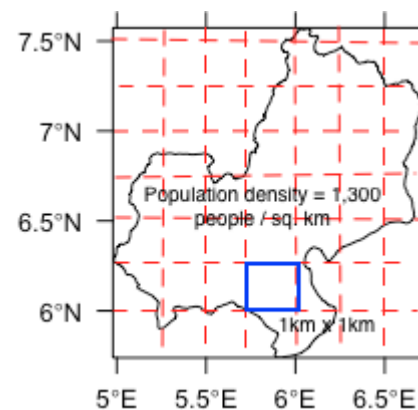


FIGURE 4. Illustrates the scaled down area of Benin.

ering the output generated through $\text{ABM}_{(1\text{km} \times 1\text{km})}$ and $\text{ABM}_{(3\text{km} \times 3\text{km})}$, then comparing against the actual reported cases. A small sample *t-test* [55]–[57] of two-independent samples was used to test the null hypothesis that on average the ABM output and reported cases are the same, at precision level $\alpha = 5\%$. The results show that no sufficient evidence to reject the null hypothesis as p -value = 0.1157 and 0.4549 for the scales, $1\text{km} \times 1\text{km}$ and $3\text{km} \times 3\text{km}$ respectively. Hence, the choosing of optimal scale is determined by minimal estimate of the associated standard error, which are $s.e.(1\text{km} \times 1\text{km}) = 97.59$ and $s.e.(3\text{km} \times 3\text{km}) = 128.37$. This is further confirmed by the observed positive correlation [58]–[60] between the ABM's results ($r_{(1\text{km} \times 1\text{km})} = 0.8$ and $r_{(3\text{km} \times 3\text{km})} = 0.5$) and reported cases. As shown in Figure 2, the scale $1\text{km} \times 1\text{km}$ is used for Tripura, then $3\text{km} \times 3\text{km}$ and $1\text{km} \times 1\text{km}$ for Limpopo and Benin City respectively.

D. PARAMETRISATION

Among other factors that influenced malaria transmission, this study focuses primarily on climatic factors. In particular, the temperature is a major driver of malaria transmission [9]. As shown in Figure 1, mosquito-related parameters, such as the mosquito biting rate $c_m(T)$, adult mosquito mortality rate $\mu_m(T)$, immature mosquito mortality rate $\mu_a(T)$ and

TABLE 2. Demographic information of the study areas.

| | Cities | | |
|---------------------|------------------------|------------------------|----------------------|
| | Tripura District, 2011 | Limpopo Province, 2015 | Benin City, 2011 |
| Population size | 3,673,917 | 5,554,657 | 1,495,800 |
| Land area | 10,492km ² | 125,754Km ² | 1,204Km ² |
| Arable land | 6,085/km ² | 88,028/km ² | 338/km ² |
| Population density | 350/km ² | 44/Km ² | 1242/Km ² |
| Physiologic density | 600/km ² | 60/km ² | 4000/km ² |
| Target population | 350 | 400 | 1300 |
| Life Expectancy | 69 | 62.77 | 54.5 |

adult mosquito egg deposition rate $\alpha_E(T)$, all depend on temperature. Since there was no empirical evidence or values of these temperature-dependent parameters for the cities selected, the functional relationship between these parameters in [38] were utilised to determine the precise values corresponding to the demographic and climate information in Table 2. The temperature-dependent function of the parameters was described using the polynomial of degree two. Their mathematical representations are shown in Equation 5.

$$\begin{aligned} c_m(T) &= -0.00014T^2 + 0.027T - 0.322 \\ \mu_m(T) &= -\ln(-0.000828T^2 + 0.0367T + 0.522) \quad (5) \\ \alpha_E(T) &= -0.153T^2 + 8.61T - 97.7 \end{aligned}$$

Also, the temperature-dependent linear function describing immature mosquito mortality rate is defined in [61], given by

$$\mu_a(T) = \frac{1}{[8.560 + 20.654[1 + (\frac{T}{19.759})^{6.827}]^{-1}]} \quad (6)$$

Using the temperature records of these cities (see [48] for Tripura district and [62] for Limpopo province and Benin city), we can obtain the values of the temperature-dependent parameters, which are presented in Table 3. These values are used in our simulations. Other parameters, e.g., the human birth or recruitment rate η , and the per capita human death rate μ_h , can be calculated using the population size and human life expectancy of the cities (see Table 2). This information was accessed in the census database of the cities through online published sources (following the references [63]–[67]). The formulas used for computing the human birth and death rates are $\eta = \mu_h \times N$ and $\mu_h = 1/(LE \times I)$, where N is the total human population size, LE is the human life expectancy and I is the index denoting the rate per month or day [68].

E. SIMULATION TOOLKITS

Two simulation platforms were used: *VenSim* [71] for mathematical modelling and *NetLogo* [72] for agent-based modelling. Agent-based models can also be implemented using programming languages such as *C*, *Java* and *Python*. *C* programming language was used to develop the *Repast*, *Soar* and *Swarm* platforms. These platforms are primarily designed for social sciences, general learning problems and general-purpose agent-based systems, respectively [73]. *Java* is, on the other hand, a versatile programming language used in building many platforms, including *AnyLogic*, *Cougar*, *JADE*, *MASON*, *Repast*, *SARL*, *Soar*, *Sugarscape*

and *Swarm*. In *Python*, agent-based models are implemented in a framework called *Mesa*, which is a modular framework for constructing, analysing and viewing agent-based models [74].

IV. EXPERIMENTATION

In this section, we present our experiments carried out using mathematical and agent-based modelling based on the malaria model shown in Figure 1. A system dynamics model in the *VenSim* platform was used to design the causal loop diagram shown in Figure 8, and the simulation of the malaria transmission model is shown in Figure 1. The *NetLogo* platform was subsequently utilized for agent-based modelling and simulation by tuning the values of the parameters in Table 3, such as average temperature, population size, land mass, density, and human life expectancy. A detailed discussion of the experiments and processes is provided below:

A. VENSIM SIMULATION

The diagram in Figure 5, generated using the *VenSim* system dynamic modeller, is a causal loop representation of the model shown in Figure 1. The values of the parameters in Table 3 were selected and referenced to the cities' climate and demographic information and supplied within the system dynamic modeller's causal loop diagram on the *VenSim* platform (see Figure 5). Subsequently, the model was calibrated, and the results were simulated within the ranges of the parameters to generate the dynamics of malaria transmission for each of the cities. The results obtained for each city are presented in Table 4 and depicted in Figures 10–12.

A numerical solution of mathematical modelling is a deterministic or non-probabilistic outcome in which, within a particular set of parameters, the results of the simulation remain consistent for any number of trials. However, in agent-based modelling, every trial of a simulation from the same set of parameters can lead to considerably different outcomes.

B. NETLOGO SIMULATION

The *NetLogo* platform captures all mobile agents, such as humans and mosquitos, as *turtles* and static agents, such as the environment, *patches* [72]. The visualization dashboard provided in this platform is not sufficient to illustrate the number of human and mosquito agents. Therefore, in our experiments, we used rescaled agent populations within the demarcated areas of the cities, as indicated in Figures 2–4. Similarly, the mosquito population used for the simulation was difficult to determine because they were uncountable and difficult to control. However, a 1:2 ratio is often used for the human-to-mosquito population (as suggested by [6], [44]). In *NetLogo*, we used 1:40 mosquitoes, where one real-shaped mosquito represented 40 virtual mosquitoes. Figure 6 presents the initial setup of the agent-based model simulation interface of the malaria transmission model shown in Figure 1. To realistically mimic human and mosquito disposition in an actual environment, we spatially distributed all the

TABLE 3. The parameter values and their ranges.

| Symbol | Baseline | Range | Reference |
|-------------|----------------------------------|--|-----------------|
| η | $4 \times 10^{-5}/\text{day}$ | $(3.91 - 5) \times 10^{-5}/\text{day}$ | [6] |
| ω_h | $1.7 \times 10^{-5}/\text{day}$ | $5.5 \times 10^{-5} - 1.1 \times 10^{-2}/\text{day}$ | [8] |
| μ_h | $4 \times 10^{-5}/\text{day}$ | $(3.42 - 3.91) \times 10^{-5}/\text{day}$ | [8] |
| μ_m | $5 \times 10^{-2}/\text{day}$ | $(4.76 - 7.14) \times 10^{-2}/\text{day}$ | [8], [69] |
| μ_a | $1.04 \times 10^{-1}/\text{day}$ | $1 \times 10^{-3} - 2 \times 10^{-1}/\text{day}$ | [4], [8], [68] |
| α_E | 1.84/day | 1 – 500/day | [4], [8], [68] |
| p | 0.25 | - | [6] |
| α_h | 5×10^{-3} | $(2 - 7) \times 10^{-3}$ | [4] |
| γ_h | $2.3 \times 10^{-3}/\text{day}$ | $1.4 \times 10^{-3} - 1.7 \times 10^{-2}/\text{day}$ | [8] |
| θ_m | $9.1 \times 10^{-2}/\text{day}$ | $2.9 \times 10^{-2} - 3.3 \times 10^{-1}/\text{day}$ | [8] |
| τ_2 | 10 | 10 – 14/days | [9] |
| a | $2.4 \times 10^{-1}/\text{day}$ | $7.2 \times 10^{-2} - 6.4 \times 10^{-1}/\text{day}$ | [4], [69], [70] |
| b | $2.2 \times 10^{-2}/\text{day}$ | $2.7 \times 10^{-3} - 6.4 \times 10^{-1}/\text{day}$ | [4], [8], [70] |
| c_m | 0.29/day | 0.10 – 1.0/day | [4], [69], [70] |
| m | 2 | - | [6] |
| ϕ_{EA} | 0.343/day | 0.333 – 1.0 | [4] |
| K_c | 4×10^4 | 50 – 3.3×10^6 | [4], [8] |
| τ_1 | 12 | 10 – 37days | [4], [38] |
| δ_h | 3.454×10^{-4} | 0 – $4.1 \times 10^{-4}/\text{day}$ | [8] |

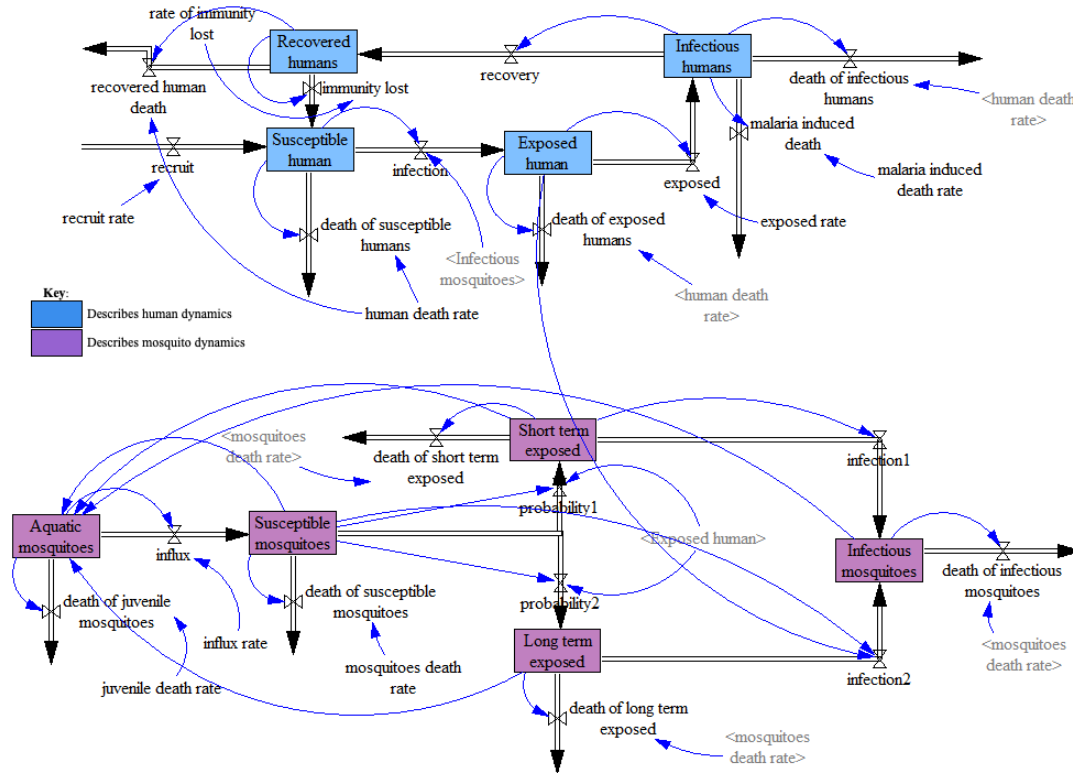


FIGURE 5. Simulation of the model in Figure 1 using Vensim system dynamic modeller.

agents in the *NetLogo* environment. Sliders and plotting spaces were used as the simulation parameters and outputs, respectively. Subsequently, for human ratio 1:35, we used human to mosquito ratio to be 35:70, and then represent 70 mosquitoes in the ratio 1:5 to get the rescale simulation ratio to be 35:14. Similarly, the ratio 1:4 and 1:13 are computed to get the rescale ratio to be 44:22 and 65:26 respectively.

1) Creating Environment

The *NetLogo* setup for the agent-based model of malaria transmission, as shown in Figure 1, is shown in Figure 6. We created three *NetLogo* objects: environment (ask patches [set pcolor green]), human agents, and mosquito agents. Human and mosquito agents are depicted in *person* and *butterfly* shapes, respectively. Subse-

quently, human and mosquito agents were initialized by their spatial dispositions in the environment by invoking [random-xcor, random-ycor] to account for systematic preferences during the simulation. To initiate malaria transmission within the created small environment, we assumed that few human agents have a malaria infection in their blood, and humans are hosts of the pathogens causing malaria [75], called *Plasmodium species*. Hence, for malaria to spread effectively in the environment, we made the following assumptions:

- i. 10% of the human agents are infected with malaria.
- ii. All mosquitoes were adults and susceptible at the initial time. Assuming that 10% of the human agents have malaria infection, we used red colour to distinguish infected human agents and to avoid bewild in the susceptible counterparts.

We then invoked the following command to ask that 10% of the human agents become infected and are assigned a red colour (if random-float initial-number-of-humans < 10). The remaining human agents were healthier and maintained their white colour, as shown in Figure 6. Because all agents were displaced randomly in the created *NetLogo* environment, the next step was to define the sets of rules or instructions for the agents to follow and behave accordingly.

2) Agents Procedure

The spread of malaria depends on the extent to which the agents interact. People move from one place to another for several reasons such as school, work, business, or tourism. Such movements increase the risk of infection. Therefore, we assumed that agents would travel through the *NetLogo* environment to spread malaria infection (see Figure 7) regardless of the reason for their movement. The procedure (right-turn random 360°, left-turn random 360° and forward 1) accounts for the agent movements. Subsequently, if any of the mosquitoes come into contact with red-coloured humans, as the interaction progresses, the particular mosquito will then change to a blue colour (see Figure (see Figure 7)), indicating that it is infected. Infected mosquitoes will not be able to transmit malaria to susceptible humans until it completes their extrinsic incubation period (EIP). This period mostly lasts for approximately 7-14 days [76]; sometimes, mosquito and parasite species could also be another factor affecting the EIP. When the EIP is completed, the infected mosquito will then change colour to black (see Figure 7), indicating infection, and thus, it becomes a potential candidate for the spread of malaria. The aftermath is the spread of the malaria infection to the white human upon successful contact and bites by infectious mosquitoes. Consequently, infectious mosquitoes collect human blood for nourishment and egg production. Regardless of whether the mosquito is infected or infectious, both will deposit eggs around swamp areas or water bodies, and thus, new

mosquitoes will be recruited (hatch new-mosquito [set colour yellow forward 1]).

Algorithms The algorithms show the simulation steps of the malaria transmission model for human and mosquito agents.

Algorithm 1 Simulation steps for the human agents

```

1: let initial human population be  $i$ 
2: select 10% random-float of  $i$  and assign colour red
3: if 10% of  $i$  with colour red then
4:   set status infected
5: else
6:   if  $i$  coloured white then
7:     set status susceptible
8:     for( $i$  in 1: $n$ )
9:       set  $i$  to move random left or random right at 360°
10:    repeat step 3, for each iteration
11:    then step 8
12:  end if
13: end if

```

The setup has the following three components:

- i. The main environment is a world where all agents are spatially distributed.
- ii. Three plane frames were used to plot the simulation outputs in real-time as the agents interacted in the environment according to predefined rules.
- iii. Sliders and buttons were used to interact with the agents through the calibration of the model parameters and start/run.

3) Testing veracity of the ABM

To test the agent-based model shown in Figure 6, we performed a trial simulation 50 times by varying the referenced parameters of the sliders. We observed the pattern it produces through plotting spaces, while all agents communicate with each other in the environment according to predefined rules. The plots shown in Figures 7–9 describe the pattern of infectiousness in humans and mosquitoes, and susceptible human dynamics, respectively. The hypothetical values of the parameters were calibrated in the sliders to test the veracity of the agent-based model to the malaria transmission model, as shown in 1. The pattern shown in Figures 7–9 depicts the general characteristics of the behaviour of an epidemic model [77].

As the season of malaria transmission usually falls within a year, depending on the length of the rainfall season, we pre-set the simulation to run for a year to spot the peak of the malaria season. In Figure 7, a unimodal peak season is connected to a period of abundance for mosquitoes, and Figure 8 corroborates this. The results shown in Figures 7 and 8 further prove that the incidence of malaria is largely influenced by the availability of adult mosquitoes [61].

In a population with relatively low fertility and mortality rates, the pattern of malaria susceptibility in humans decreases as the infection increases. Thus, Figure 9 confirms

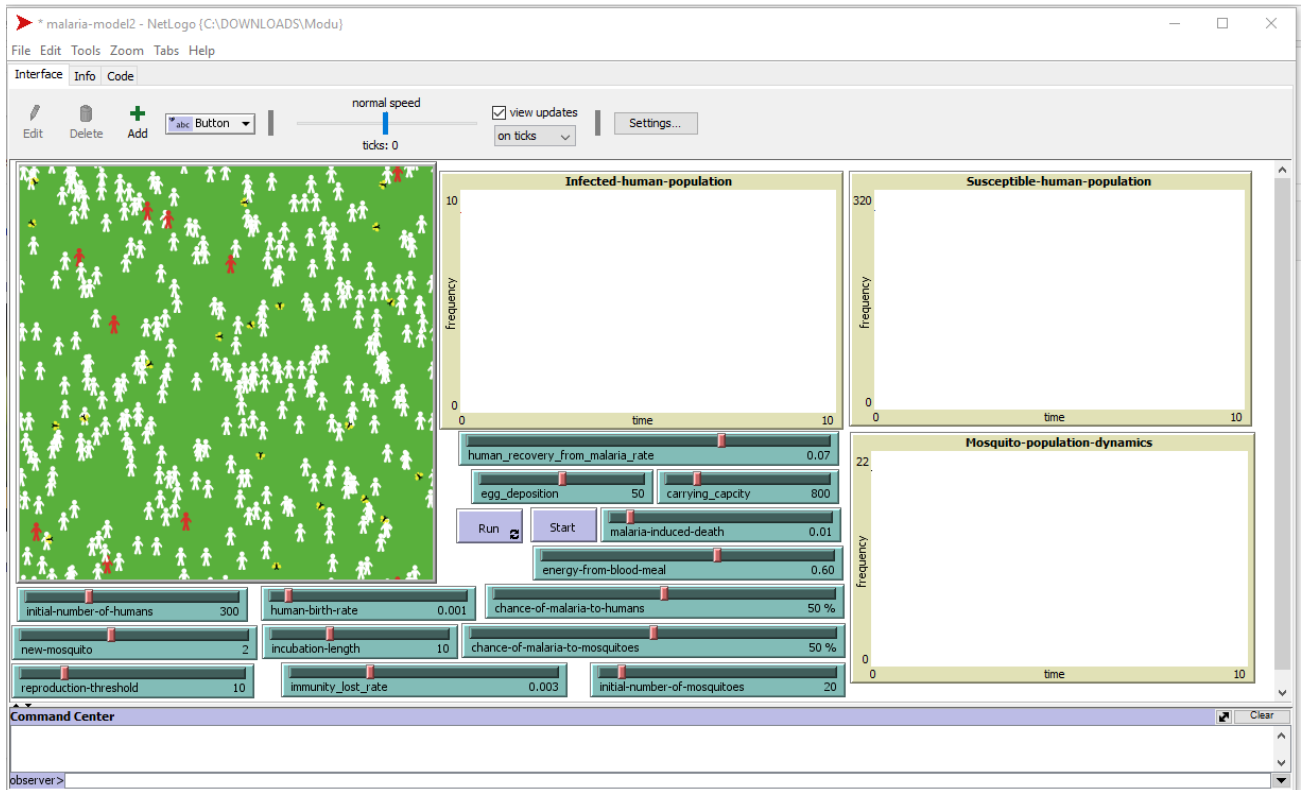


FIGURE 6. A screenshot showing the interface of the ABM using the *NetLogo* platform.

that the susceptible human population shows a decreasing pattern as time increases. This shows the robustness of an agent-based model in its ability to study the characteristics of individual agents involved in the phenomena and mimic its real-world scenario.

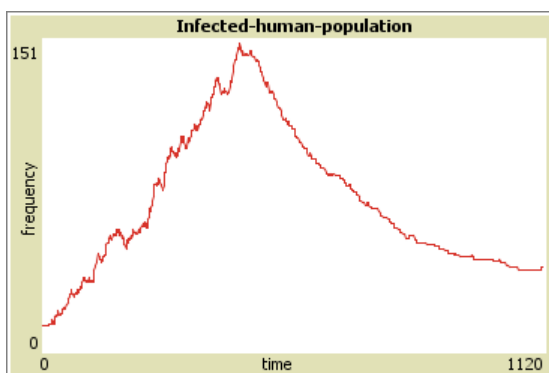


FIGURE 7. This plots show pattern of malaria's infectiousness.

By tweaking the values of the parameters within their ranges (Table 3) and concerning the cities' climates and demographic information, the pattern of malaria transmission can be resolved. For each city, we performed 100 runs of the simulation and produced results on an average of the entire simulation cycle.

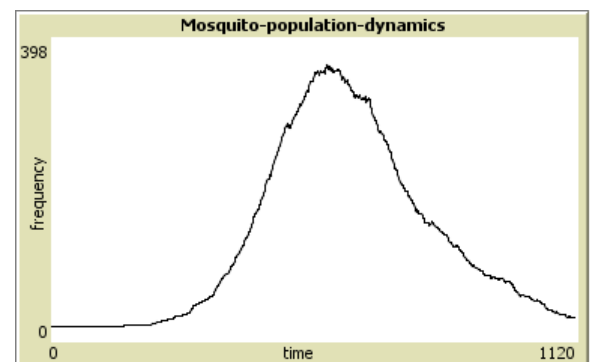


FIGURE 8. This plots show pattern of malaria's mosquito dynamics.

V. EXPERIMENTAL RESULTS AND VALIDATION

This section presents the results of the simulation model in Figure 1 using the proposed approach. For each city, we provided detailed results (see Table 4) and visualized them accordingly (see Figures 10–12). The reported cases of malaria within the cities and model results are presented in Table 4. By looking at the patterns of the results compared with the cases, we noticed high variability, as indicated by the magnitude of the values. This made it difficult to critically comprehend the patterns. However, to make them consistent because no zero instances were observed, a logarithmic transformation [78] technique was applied to normalize the results

Algorithm 2 Simulation steps for the mosquito agents

```

1: let initial mosquito population be  $j$ 
2: all  $j$ 's are assumed susceptible
3: for ( $j$  in 1:n)
4: set  $j$  to fly random left or random right at  $360^\circ$  seeking  $i$ 's blood
5: if any ( $j$  in 1:m) bite any ( $i$  in 1:n) with colour red then
6:   set status infected for  $j$ 
7:   set colour blue
8:   repeat step 5
9: else
10:  if status is susceptible then
11:    otherwise step 12
12:    for ( $j$  in 1:m) with status infected undergo extrinsic incubation period
13:  else
14:    if step 12 is completed then
15:      set status infectious
16:      set colour black
17:      repeat step 12
18:      repeat step 3 to 4 through step 14 until all  $j$ 's are infectious
19:      let  $\lambda$  be the average lifespan for  $j$ 's
20:    else
21:      if lifespan for each  $j$ 's in step 18 exceed  $\lambda$  then
22:        set status die
23:        repeat step 3
24:      else
25:        if all  $j$ 's execute step 21 to 22 then
26:          stop
27:        end if
28:      end if
29:    end if
30:  end if
31: end if

```

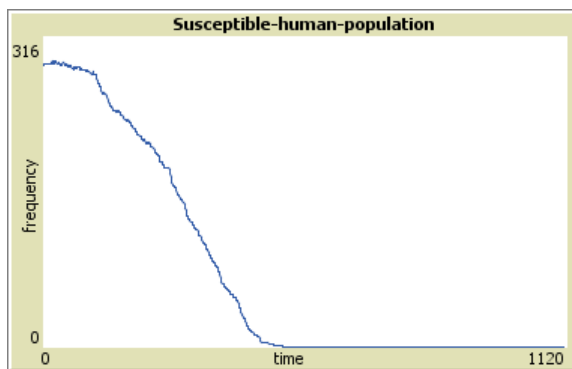


FIGURE 9. This plots show pattern of malaria's human susceptibility.

in Table 4. The log-transformed values in Table 4 are plotted in Figures 10–12.

Figure 10 presents the cases of malaria reported in the Tripura district against the model results produced using

an agent-based model and a mathematical model (see Table 4). The plots were produced using the two modelling approaches and indicated a certain strength of relationship within the occurrences of malaria in the district. The peak season of malaria incidence was predicted, as evidenced by the fluctuation produced using modelling approaches, which is similar to the cases reported. Agent-based modelling and mathematical modelling performed well in predicting not only the pattern of malaria transmission in the district but also the season.

Similarly, Figure 11 shows a comparison between the cases of malaria reported in the Limpopo province and the model-generated results using an agent-based model and mathematical model (Table 4). The pattern produced by the plots in Figure 11 clearly shows that malaria occurrences in the province are well represented using the agent-based model results. However, the results produced using the mathematical model mimicked the pattern of the provincial malaria cases at the beginning of the simulation but later drifted down. This is because mathematical models are suitable for trend analysis and investigating continuous phenomena. Hence, between the two modelling approaches, the agent-based model performed better in predicting the pattern of malaria incidence in the province.

Figure 12 presents plots of the reported cases of malaria in Benin City, together with the simulation results generated through an agent-based model and mathematical model (see Table 4). The plots in Figure 12 show that the agent-based model works better in predicting the fluctuating behaviour of reported malaria cases. However, the mathematical model produces a trend that fails to capture fluctuations. This shows that mathematical modelling is a good candidate for trend analysis but not for capturing a fine-grained relationship.

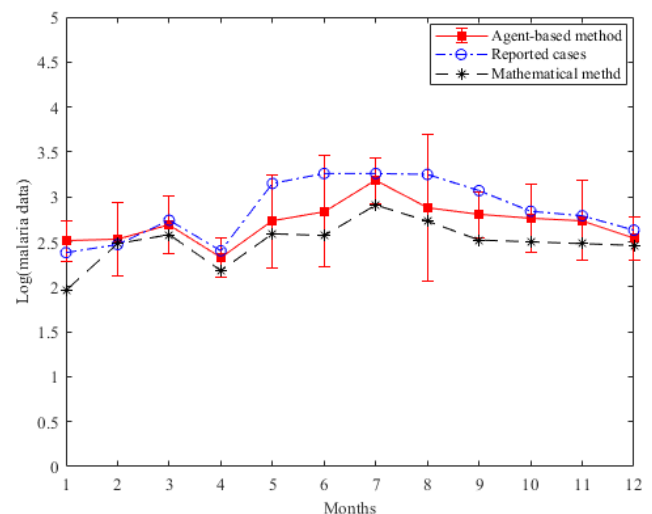


FIGURE 10. The plots showing reported cases of malaria against model-generated cases for Tripura.

TABLE 4. Reported cases of malaria in the three cities and the simulated results.

| Months | Cities | | | | | | | | | | | | | | | | | |
|--------|------------------------|--------|------|--------|-----|--------|------------------------|--------|-----|--------|----|--------|------------------|--------|------|--------|------|--------|
| | Tripura district, 2011 | | | | | | Limpopo province, 2015 | | | | | | Benin city, 2011 | | | | | |
| | C | log(C) | A | log(A) | M | log(M) | C | log(C) | A | log(A) | M | log(M) | C | log(C) | A | log(A) | M | log(M) |
| Jan | 240 | 2.38 | 320 | 2.51 | 91 | 1.96 | 863 | 2.94 | 293 | 2.47 | 33 | 1.52 | 58 | 1.76 | 133 | 2.12 | 28 | 1.45 |
| Feb | 298 | 2.47 | 337 | 2.53 | 300 | 2.48 | 1843 | 3.27 | 594 | 2.77 | 61 | 1.79 | 110 | 2.04 | 191 | 2.28 | 134 | 2.13 |
| Mar | 552 | 2.74 | 493 | 2.69 | 384 | 2.58 | 1588 | 3.20 | 341 | 2.53 | 43 | 1.63 | 199 | 2.30 | 219 | 2.34 | 251 | 2.40 |
| Apr | 254 | 2.40 | 210 | 2.32 | 152 | 2.18 | 411 | 2.61 | 143 | 2.16 | 15 | 1.18 | 258 | 2.41 | 268 | 2.43 | 377 | 2.58 |
| May | 1398 | 3.15 | 538 | 2.73 | 388 | 2.59 | 85 | 1.93 | 143 | 2.16 | 09 | 0.95 | 534 | 2.73 | 324 | 2.51 | 523 | 2.72 |
| Jun | 1817 | 3.26 | 699 | 2.84 | 374 | 2.57 | 38 | 1.58 | 113 | 2.05 | 06 | 0.78 | 512 | 2.71 | 251 | 2.40 | 686 | 2.84 |
| Jul | 1833 | 3.26 | 1520 | 3.18 | 812 | 2.91 | 25 | 1.40 | 51 | 1.71 | 04 | 0.60 | 396 | 2.60 | 134 | 2.13 | 848 | 2.93 |
| Aug | 1760 | 3.25 | 750 | 2.88 | 543 | 2.73 | 49 | 1.69 | 142 | 2.15 | 03 | 0.48 | 787 | 2.90 | 610 | 2.79 | 986 | 2.99 |
| Sep | 1181 | 3.07 | 630 | 2.80 | 329 | 2.52 | 123 | 2.09 | 120 | 2.08 | 02 | 0.30 | 1092 | 3.04 | 1567 | 3.20 | 1078 | 3.03 |
| Oct | 684 | 2.84 | 575 | 2.76 | 315 | 2.50 | 192 | 2.28 | 192 | 2.28 | 02 | 0.30 | 129 | 2.11 | 720 | 2.86 | 1118 | 3.05 |
| Nov | 614 | 2.79 | 554 | 2.74 | 302 | 2.48 | 144 | 2.16 | 201 | 2.30 | 02 | 0.30 | 201 | 2.30 | 675 | 2.83 | 1111 | 3.05 |
| Dec | 431 | 2.63 | 347 | 2.54 | 289 | 2.46 | 83 | 1.92 | 132 | 2.12 | 02 | 0.30 | 54 | 1.73 | 112 | 2.05 | 1074 | 3.03 |

where: C = Reported cases of malaria, A = Agent-based results, M = Mathematical results and log(C), log(A), log(M) are their logarithmic transformed.

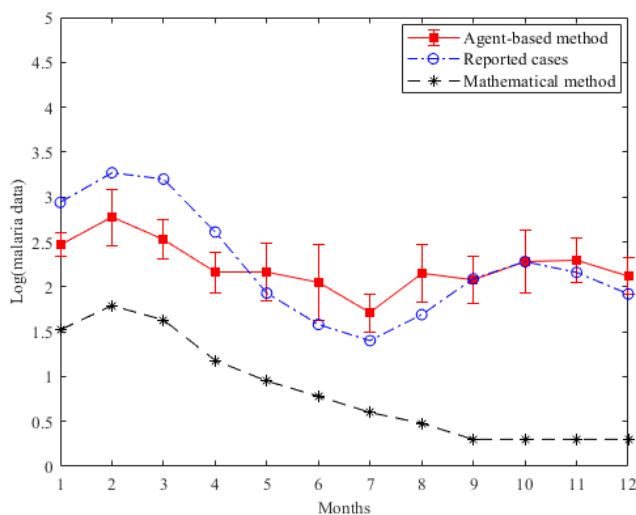


FIGURE 11. The plots showing reported cases of malaria against model-generated cases for Limpopo.

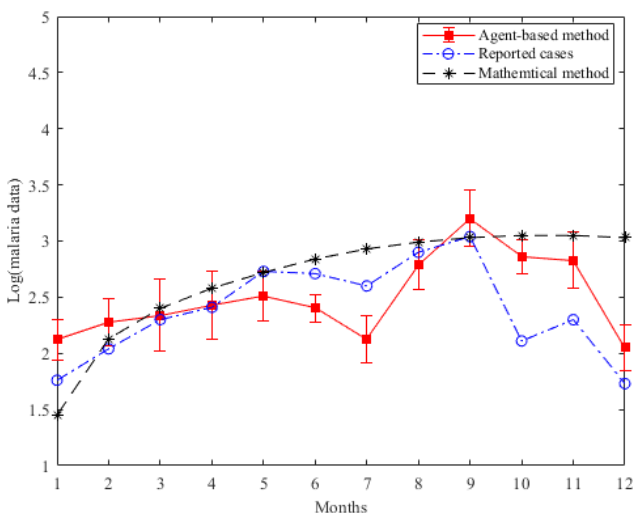


FIGURE 12. The plots showing reported cases of malaria against model-generated cases for Benin.

A. STATISTICAL TESTS AND INFERENCES

The plots in Figures 10–12 demonstrate a pattern that means that it is difficult to recognize the best performing model

in predicting the occurrence of malaria between the agent-based and mathematical models. A *t-test* for two independent samples [55], together with a *correlation coefficient* [58], [59], was utilized, and the best-performing model was selected. The computational results of the parameters for the two statistical techniques are summarized in Table 5.

TABLE 5. Present the summarised results of the *t-test* for two independent samples.

| t-statistic | Cities | | | | | | | | |
|-------------|------------------|--------|--------|------------------|--------|--------|------------|--------|--------|
| | Tripura district | | | Limpopo province | | | Benin city | | |
| t-value | 1.6378 | 2.9560 | 2.0222 | 1.3444 | 2.3861 | 4.4766 | 0.0850 | 3.4243 | 1.4874 |
| p-value | 0.1157 | 0.0073 | 0.0274 | 0.1925 | 0.0261 | 0.0001 | 0.9330 | 0.0084 | 0.0276 |
| r | 0.7732 | 0.7768 | - | 0.9784 | 0.9318 | - | 0.7176 | 0.5420 | - |
| Remark | Not sign | Sign | Sign | Not sign | Sign | Sign | Not sign | Sign | Sign |

where: t-value = test-statistic, p-value = highest threshold probability for rejecting the null hypothesis, r = coefficient of correlation used to measure a degree of association, Not sign = indicating there is no significant difference and Sign = indicating there is a significant difference.

Based on the results presented in Table 5, Figure 10 shows that there is no significant difference on average between the reported cases of malaria and the simulation results produced through an agent-based model ($p - value = 0.1157 > \alpha = 0.05$). Similarly, it is also observed that there is a significant difference in the results produced through the mathematical model compared to the reported cases of malaria in Tripura ($p - value = 0.0073 < \alpha = 0.05$). A moderate degree of association was found (see Table 5, $r = 0.7732$ and $r = 0.7768$) between the reported cases of malaria and the model-based results produced using the agent-based and mathematical models, respectively. The results in Table 5 affirmed no significant difference between the reported cases of malaria and the results produced using the agent-based model in Limpopo and Benin ($p - value = 0.1925 > \alpha = 0.05$ and $p - value = 0.9330 > \alpha = 0.05$ respectively). However, the mathematical modelling results were found to be significantly different from the malaria cases reported in the two cities ($p - value = 0.0261 < \alpha = 0.05$ and $p - value = 0.0084 < \alpha = 0.05$ respectively). Furthermore, a strong correlation between the malaria cases in Limpopo and the agent-based model cases was found ($r = 0.9784$ in Table 5), and this result was also similar to those produced by the mathematical model ($r = 0.9318$ in Table 5). However, in Benin, the degree of association between the cases of

malaria and the results produced using the agent-based model was moderately good compared to the mathematical model ($r = 0.7176$ and $r = 0.5420$ respectively).

In all the cities studied, the agent-based model performed well in predicting the occurrence of malaria incidence, as opposed to the mathematical model. However, the mathematical model was good for trend analysis and performed particularly well for Tripura and Benin (see Figures 10–12) compared with Limpopo (see Figure 11).

VI. CONCLUSION

Employing an accurate tool to predict malaria outbreak season would enable better planning interventions, prevention, and control, thus mitigating the human burden. This paper presents an approach that addresses the limitations of the mathematical modelling approach by proposing an agent-based technique to investigate malaria transmission. The agent-based model was simulated and validated against hospital-reported cases and then compared with the results generated by the mathematical model, which was used as a benchmark. Through analysis, we observed that the agent-based model proved to be better at predicting the season of malaria and the possible fluctuations in the reported cases. Our study shows that agent-based models can capture heterogeneity better and provide more detailed information, such as where an agent becomes infected. Our model can be generalized to study malaria transmission at different locations by tweaking location-specific demographic and climate-dependent parameters. This information could lead to a better understanding of the spread of malaria, allowing public health organizations to focus on specific areas or contact tracking. Furthermore, our results can help healthcare providers and policymakers with a tool showing how malaria invades the population, thus planning for prevention and control. Our future work will extend the agent-based model studied to investigate human movement patterns and mosquito breeding sites.

COMPETING INTERESTS

The authors declare that they have no competing interests.

AUTHOR'S CONTRIBUTIONS

Babagana Modu, Nereida Polovina, and Savas Konur designed the experiments; Babagana Modu performed the experiments and analyzed the data; Babagana Modu, Nereida Polovina, and Savas Konur analyzed and evaluated the results; Babagana Modu wrote the paper, and all authors edited the paper.

ACKNOWLEDGEMENTS

B. Modu acknowledges the Tertiary Education Trust Fund (TetFund) Nigeria (in collaboration with Yobe State University Damaturu) for sponsoring his PhD studies at the University of Bradford. The work of S. Konur was supported by EPSRC (EP/R043787/1).

REFERENCES

- [1] A. Online, World malaria report 2107: World health organization, 2017.
- [2] W. H. Organization et al., World malaria report 2022. World Health Organization, 2022.
- [3] K. Twum-Nuamah, "World malaria day," 2019.
- [4] K. Okuneye and A. B. Gumel, "Analysis of a temperature-and rainfall-dependent model for malaria transmission dynamics," *Mathematical biosciences*, vol. 287, pp. 72–92, 2017.
- [5] K. Okuneye, A. Abdelrazec, and A. B. Gumel, "Mathematical analysis of a weather-driven model for the population ecology of mosquitoes," *Mathematical Biosciences & Engineering*, vol. 15, no. 1, p. 57, 2018.
- [6] K. Nah, Y. Nakata, and G. Röst, "Malaria dynamics with long incubation period in hosts," *Computers & Mathematics with Applications*, vol. 68, no. 9, pp. 915–930, 2014.
- [7] L.-F. Nie and Y.-N. Xue, "The roles of maturation delay and vaccination on the spread of dengue virus and optimal control," *Advances in Difference Equations*, vol. 2017, no. 1, pp. 1–19, 2017.
- [8] F. Agosto, A. Gumel, and P. Parham, "Qualitative assessment of the role of temperature variations on malaria transmission dynamics," *Journal of Biological Systems*, vol. 23, no. 04, p. 1550030, 2015.
- [9] K. P. Paaijmans, A. F. Read, and M. B. Thomas, "Understanding the link between malaria risk and climate," *Proceedings of the National Academy of Sciences*, vol. 106, no. 33, pp. 13844–13849, 2009.
- [10] L. L. Shapiro, S. A. Whitehead, and M. B. Thomas, "Quantifying the effects of temperature on mosquito and parasite traits that determine the transmission potential of human malaria," *PLoS biology*, vol. 15, no. 10, p. e2003489, 2017.
- [11] S. A. Herzog, S. Blaizot, and N. Hens, "Mathematical models used to inform study design or surveillance systems in infectious diseases: a systematic review," *BMC infectious diseases*, vol. 17, no. 1, pp. 1–10, 2017.
- [12] L. Kong, J. Wang, W. Han, and Z. Cao, "Modeling heterogeneity in direct infectious disease transmission in a compartmental model," *International journal of environmental research and public health*, vol. 13, no. 3, p. 253, 2016.
- [13] Q. Zhang, K. Sun, M. Chinazzi, A. Pastore y Piontti, N. E. Dean, D. P. Rojas, S. Merler, D. Mistry, P. Poletti, L. Rossi, et al., "Spread of zika virus in the americas," *Proceedings of the national academy of sciences*, vol. 114, no. 22, pp. E4334–E4343, 2017.
- [14] H. Ullah, W. Wan, S. A. Haidery, N. U. Khan, Z. Ebrahimpour, and A. Muzahid, "Spatiotemporal patterns of visitors in urban green parks by mining social media big data based upon who reports," *IEEE Access*, vol. 8, pp. 39197–39211, 2020.
- [15] P. He, A. A. Maldonado-Chaparro, and D. R. Farine, "The role of habitat configuration in shaping social structure: a gap in studies of animal social complexity," *Behavioral Ecology and Sociobiology*, vol. 73, no. 1, pp. 1–14, 2019.
- [16] H. Barbosa, M. Barthelemy, G. Ghoshal, C. R. James, M. Lenormand, T. Louail, R. Menezes, J. J. Ramasco, F. Simini, and M. Tomasini, "Human mobility: Models and applications," *Physics Reports*, vol. 734, pp. 1–74, 2018.
- [17] D. L. Chao, M. E. Halloran, V. J. Obenchain, and I. M. Longini Jr, "Flute, a publicly available stochastic influenza epidemic simulation model," *PLoS computational biology*, vol. 6, no. 1, p. e1000656, 2010.
- [18] J. Hackl and T. Dubernet, "Epidemic spreading in urban areas using agent-based transportation models," *Future internet*, vol. 11, no. 4, p. 92, 2019.
- [19] N. R. Smith, J. M. Trauer, M. Gambhir, J. S. Richards, R. J. Maude, J. M. Keith, and J. A. Flegg, "Agent-based models of malaria transmission: a systematic review," *Malaria journal*, vol. 17, no. 1, pp. 1–16, 2018.
- [20] L. Willem, F. Verelst, J. Bilcke, N. Hens, and P. Beutels, "Lessons from a decade of individual-based models for infectious disease transmission: a systematic review (2006-2015)," *BMC infectious diseases*, vol. 17, no. 1, pp. 1–16, 2017.
- [21] B. Modu, N. Polovina, Y. Lan, and S. Konur, "Machine learning analysis and agent-based modelling of malaria transmission," in *Fuzzy Systems and Data Mining IV*, pp. 465–472, IOS Press, 2018.
- [22] M. Amadi, "Hybrid modelling methods for epidemiological studies," 2022.
- [23] A. McAlpine, L. Kiss, C. Zimmerman, and Z. Chalabi, "Agent-based modeling for migration and modern slavery research: a systematic review," *Journal of computational social science*, vol. 4, no. 1, pp. 243–332, 2021.
- [24] M. Amadi, A. Shcherbacheva, and H. Haario, "Agent-based modelling of complex factors impacting malaria prevalence," *Malaria journal*, vol. 20, no. 1, pp. 1–15, 2021.

- [25] B. Modu, A Holistic Approach to Dynamic Modelling of Malaria Transmission. An Investigation of Climate-Based Models used for Predicting Malaria Transmission. PhD thesis, University of Bradford, 2020.
- [26] O. Koutou, B. Traoré, and B. Sangaré, "Mathematical model of malaria transmission dynamics with distributed delay and a wide class of non-linear incidence rates," *Cogent Mathematics & Statistics*, vol. 5, no. 1, p. 1564531, 2018.
- [27] S. Ruan, D. Xiao, and J. C. Beier, "On the delayed ross-macdonald model for malaria transmission," *Bulletin of mathematical biology*, vol. 70, no. 4, pp. 1098–1114, 2008.
- [28] S. Olaniyi and O. Obabiyi, "Mathematical model for malaria transmission dynamics in human and mosquito populations with nonlinear forces of infection," *International journal of pure and applied Mathematics*, vol. 88, no. 1, pp. 125–156, 2013.
- [29] S. Mandal, R. R. Sarkar, and S. Sinha, "Mathematical models of malaria-a review," *Malaria journal*, vol. 10, no. 1, pp. 1–19, 2011.
- [30] G. Macdonald et al., "The epidemiology and control of malaria," *The Epidemiology and Control of Malaria*, 1957.
- [31] J. L. Aron, "Mathematical modelling of immunity to malaria," *Mathematical Biosciences*, vol. 90, no. 1-2, pp. 385–396, 1988.
- [32] J. L. Aron and R. M. May, "The population dynamics of malaria," in *The population dynamics of infectious diseases: theory and applications*, pp. 139–179, Springer, 1982.
- [33] K. Dietz, L. Molineaux, and A. Thomas, "A malaria model tested in the african savannah," *Bulletin of the World Health Organization*, vol. 50, no. 3-4, p. 347, 1974.
- [34] H. W. Hethcote, "The mathematics of infectious diseases," *SIAM review*, vol. 42, no. 4, pp. 599–653, 2000.
- [35] W. Duan, Z. Fan, P. Zhang, G. Guo, and X. Qiu, "Mathematical and computational approaches to epidemic modeling: a comprehensive review," *Frontiers of Computer Science*, vol. 9, no. 5, pp. 806–826, 2015.
- [36] H. Li, R. Peng, and Z.-a. Wang, "On a diffusive susceptible-infected-susceptible epidemic model with mass action mechanism and birth-death effect: analysis, simulations, and comparison with other mechanisms," *SIAM Journal on Applied Mathematics*, vol. 78, no. 4, pp. 2129–2153, 2018.
- [37] Z. Cao, Y. Wang, W. Zheng, L. Yin, Y. Tang, W. Miao, S. Liu, and B. Yang, "The algorithm of stereo vision and shape from shading based on endoscope imaging," *Biomedical Signal Processing and Control*, vol. 76, p. 103658, 2022.
- [38] E. A. Mordecai, K. P. Paaijman, L. R. Johnson, C. Balzer, T. Ben-Horin, E. de Moor, A. McNally, S. Pawar, S. J. Ryan, T. C. Smith, et al., "Optimal temperature for malaria transmission is dramatically lower than previously predicted," *Ecology letters*, vol. 16, no. 1, pp. 22–30, 2013.
- [39] P. Van den Driessche and J. Watmough, "Reproduction numbers and sub-threshold endemic equilibria for compartmental models of disease transmission," *Mathematical biosciences*, vol. 180, no. 1-2, pp. 29–48, 2002.
- [40] P. Van den Driessche, "Reproduction numbers of infectious disease models," *Infectious Disease Modelling*, vol. 2, no. 3, pp. 288–303, 2017.
- [41] A. Perasso, "An introduction to the basic reproduction number in mathematical epidemiology," *ESAIM: Proceedings and Surveys*, vol. 62, pp. 123–138, 2018.
- [42] W. Dubitzky, O. Wolkenhauer, K.-H. Cho, and H. Yokota, *Encyclopedia of systems biology*, vol. 402. Springer New York, 2013.
- [43] A. Nejat and I. Damnjanovic, "Agent-based modeling of behavioral housing recovery following disasters," *Computer-Aided Civil and Infrastructure Engineering*, vol. 27, no. 10, pp. 748–763, 2012.
- [44] A. Jindal and S. Rao, "Agent-based modeling and simulation of mosquito-borne disease transmission," in *Proceedings of the 16th conference on autonomous agents and multiagent systems*, pp. 426–435, 2017.
- [45] B. Modu, N. Polovina, Y. Lan, S. Konur, A. T. Asyhari, and Y. Peng, "Towards a predictive analytics-based intelligent malaria outbreak warning system," *Applied Sciences*, vol. 7, no. 8, p. 836, 2017.
- [46] B. Modu, A. T. Asyhari, S. Konur, and Y. Peng, "An assessment on the hidden ecological factors of the incidence of malaria," *Multidisciplinary Digital Publishing Institute Proceedings*, vol. 1, no. 3, p. 131, 2017.
- [47] P. W. Gething, A. P. Patil, D. L. Smith, C. A. Guerra, I. R. Elyazar, G. L. Johnston, A. J. Tatem, and S. I. Hay, "A new world malaria map: Plasmodium falciparum endemicity in 2010," *Malaria journal*, vol. 10, no. 1, pp. 1–16, 2011.
- [48] V. Dev, T. Adak, O. P. Singh, N. Nanda, and B. K. Baidya, "Malaria transmission in tripura: Disease distribution & determinants," *The Indian journal of medical research*, vol. 142, no. Suppl 1, p. S12, 2015.
- [49] L. Blumberg and J. Frean, "Malaria control in south africa-challenges and successes," *South African Medical Journal*, vol. 97, no. 11, pp. 1193–1197, 2007.
- [50] M. H. Craig, R. Snow, and D. le Sueur, "A climate-based distribution model of malaria transmission in sub-saharan africa," *Parasitology today*, vol. 15, no. 3, pp. 105–111, 1999.
- [51] S. Dawaki, H. M. Al-Mekhlafi, I. Ithoi, J. Ibrahim, W. M. Atroosh, A. M. Abdulsalam, H. Sady, F. N. Elyana, A. U. Adamu, S. I. Yelwa, et al., "Is nigeria winning the battle against malaria? prevalence, risk factors and kap assessment among hausa communities in kano state," *Malaria journal*, vol. 15, no. 1, pp. 1–14, 2016.
- [52] A. Online, *Communicable Diseases Communiqué*, 2021.
- [53] F. Adeyemo, O. Makinde, L. Chukwuka, and E. Oyana, "Incidence of malaria infection among the undergraduates of university of benin (uniben), benin city, nigeria," *The Internet Journal of Tropical Medicine*, vol. 9, no. 1, pp. 1–8, 2013.
- [54] D. M. Rhodes, M. Holcombe, and E. E. Qvarnstrom, "Reducing complexity in an agent based reaction model—benefits and limitations of simplifications in relation to run time and system level output," *Biosystems*, vol. 147, pp. 21–27, 2016.
- [55] T. K. Kim, "T test as a parametric statistic," *Korean journal of anesthesiology*, vol. 68, no. 6, pp. 540–546, 2015.
- [56] D. R. Farine and G. G. Carter, "Permutation tests for hypothesis testing with animal social network data: Problems and potential solutions," *Methods in Ecology and Evolution*, vol. 13, no. 1, pp. 144–156, 2022.
- [57] T. K. Kim and J. H. Park, "More about the basic assumptions of t-test: normality and sample size," *Korean journal of anesthesiology*, vol. 72, no. 4, pp. 331–335, 2019.
- [58] B. Modu, A. T. Asyhari, and Y. Peng, "Data analytics of climatic factor influence on the impact of malaria incidence," in *2016 IEEE Symposium Series on Computational Intelligence (SSCI)*, pp. 1–8, IEEE, 2016.
- [59] S. Liu, B. Yang, Y. Wang, J. Tian, L. Yin, and W. Zheng, "2d/3d multi-mode medical image registration based on normalized cross-correlation," *Applied Sciences*, vol. 12, no. 6, p. 2828, 2022.
- [60] D. Makowski, M. S. Ben-Shachar, I. Patil, and D. Lüdtke, "Methods and algorithms for correlation analysis in r," *Journal of Open Source Software*, vol. 5, no. 51, p. 2306, 2020.
- [61] P. E. Parham, D. Pople, C. Christiansen-Jucht, S. Lindsay, W. Hinsley, and E. Michael, "Modeling the role of environmental variables on the population dynamics of the malaria vector anopheles gambiae sensu stricto," *Malaria Journal*, vol. 11, no. 1, pp. 1–13, 2012.
- [62] A. Online, *Climate data for cities worldwide-Climate-Data.org*, 2021.
- [63] *Gauteng online data*. Accessed 17 July 2021, from: <https://en.wikipedia.org/wiki/Gauteng>, 2019.
- [64] *Life Expectancy in Benin*. Accessed online 17 July 2021, from: <https://www.worldlifeexpectancy.com/benin-life-expectancy>, 2021.
- [65] *Limpopo Population*. Accessed Online 17 July 2021, from: <http://population.city/south-africa/adm/limpopo/>, 2021.
- [66] *North Tripura District Population Census 2011-2019, Tripura literacy sex ratio and density*. Accessed Online 17 July 2021 from: <https://census2011.co.in/census/district/460-north-tripura.html>, 2021.
- [67] *Outline of Tripura*. Accessed Online 17 July 2021, from: https://en.wikipedia.org/wiki/Outline_of_Tripura, 2021.
- [68] Y. Lou and X.-Q. Zhao, "A climate-based malaria transmission model with structured vector population," *SIAM Journal on Applied Mathematics*, vol. 70, no. 6, pp. 2023–2044, 2010.
- [69] A. M. Niger and A. B. Gumel, "Mathematical analysis of the role of repeated exposure on malaria transmission dynamics," *Differential Equations and Dynamical Systems*, vol. 16, no. 3, pp. 251–287, 2008.
- [70] N. Chitnis, J. M. Cushing, and J. Hyman, "Bifurcation analysis of a mathematical model for malaria transmission," *SIAM Journal on Applied Mathematics*, vol. 67, no. 1, pp. 24–45, 2006.
- [71] *Vensim Software*. Accessed Online through: <https://vensim.com/vensim-software/>, 2021.
- [72] U. Wilensky and W. Rand, *An introduction to agent-based modeling: modeling natural, social, and engineered complex systems with NetLogo*. MIT Press, 2015.
- [73] S. Abar, G. K. Theodoropoulos, P. Lemarinier, and G. M. O'Hare, "Agent based modelling and simulation tools: A review of the state-of-art software," *Computer Science Review*, vol. 24, pp. 13–33, 2017.

- [74] M. Cardinot, C. O'Riordan, J. Griffith, and M. Perc, "Evoplex: A platform for agent-based modeling on networks," *SoftwareX*, vol. 9, pp. 199–204, 2019.
- [75] L. C. Pollitt, J. T. Bram, S. Blanford, M. J. Jones, and A. F. Read, "Existing infection facilitates establishment and density of malaria parasites in their mosquito vector," *PLoS pathogens*, vol. 11, no. 7, p. e1005003, 2015.
- [76] J. R. Ohm, F. Baldini, P. Barreaux, T. Lefevre, P. A. Lynch, E. Suh, S. A. Whitehead, and M. B. Thomas, "Rethinking the extrinsic incubation period of malaria parasites," *Parasites & vectors*, vol. 11, no. 1, pp. 1–9, 2018.
- [77] E. Bakare, "On the optimal control of vaccination and treatments for an sir-epidemic model with infected immigrants," *Journal of Applied & Computational Mathematics*, vol. 4, no. 4, 2015.
- [78] F. Changyong, W. Hongyue, L. Naiji, C. Tian, H. Hua, L. Ying, et al., "Log-transformation and its implications for data analysis," *Shanghai archives of psychiatry*, vol. 26, no. 2, p. 105, 2014.



BABAGANA MODU received both B.Sc. and M.Sc. degrees in Applied Statistics from the University of Maiduguri and Usumanu Danfodiyo University Sokoto in 2005 and 2012, respectively. He was awarded PhD in Applied Statistics by the University of Bradford in 2020. He is currently a Senior Lecturer at the Department of Mathematics and Statistics, Yobe State University Damaturu, Nigeria. His research interests include mathematical modeling, agent-based modeling, statistical

modeling, spatial data analysis, statistical quality control, and machine learning. He has regularly published in these areas and attended several conferences, workshops, and seminars.



NEREIDA POLOVINA received her PhD degree from Lancaster University Management School in 2014. She is a Senior Lecturer and a member of the Business Transformation Research Centre at Manchester Metropolitan University. Her research involves the use of advanced statistical methods and equation modelling to identify patterns and measure trends and behaviours across industries and markets. She has several articles published in interdisciplinary areas including the healthcare

industry.



SAVAS KONUR received his PhD degree in Computer Science from the University of Manchester (UK) in 2008. He is currently a Reader and the Head of the Computational Modelling Research Group at the Department of Computer Science, University of Bradford (UK). His research involves computational and data-driven modelling and interdisciplinary applications including smart systems, healthcare systems, and synthetic biology. He has published in numerous leading high-

impact factor journals and led research projects on these topics.

...